Supporting Information

Rational design of multidimensional N-doped porous carbon/MoS_2/CNTs nano-architecture hybrid for high performance lithium-sulfur batteries

Juan Ren, Yibei Zhou, Li Xia, Qiaoji Zheng, Jie Liao, Enyan Long, Fengyu Xie, Chegngang Xu, Dunmin Lin*

College of Chemistry and Materials Science, Sichuan Normal University, Chengdu 610066, China

* Corresponding author: Tel.: +86 28 84760802; Fax: +86 28 84760802; E-mail: ddmd222@sicnu.edu.cn (Dunmin Lin)

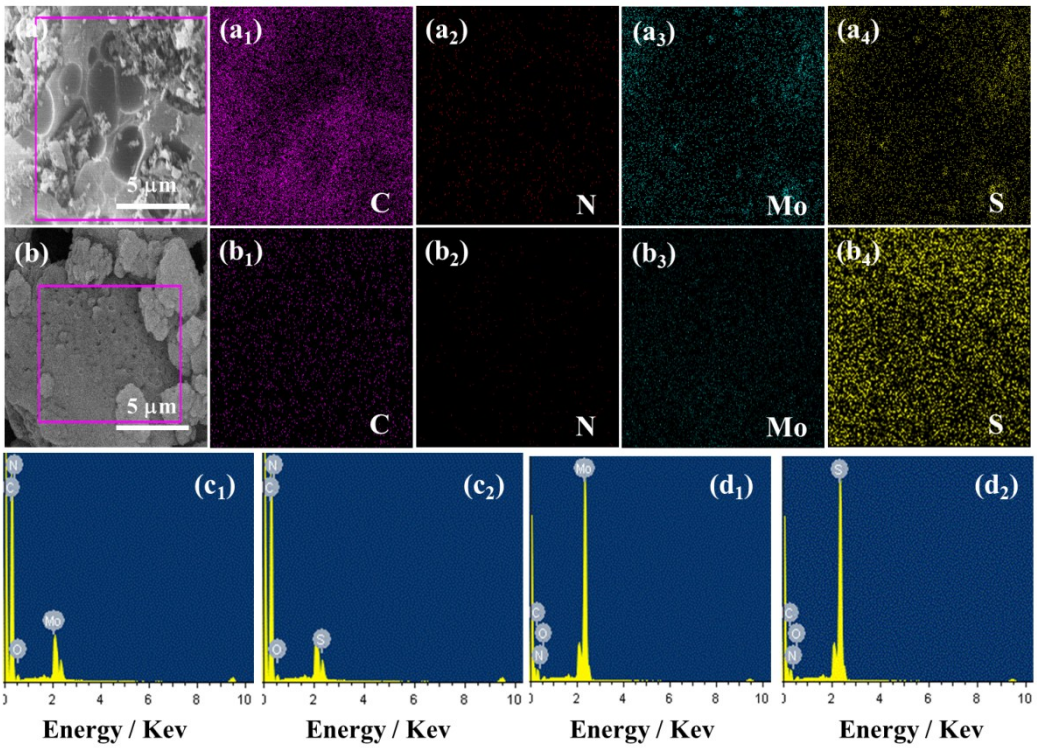

Fig. S1. FESEM image of FSC/MoS_2 (a) and the corresponding elemental mappings of C, N, Mo and S (a_1-a_4); FESEM image of FSC/MoS_2@S (b) and the corresponding elemental mappings of C, N, Mo and S (b_1-b_4); EDS spectra of FSC/MoS_2 ($c_1$and c_2) and FSC/MoS_2@S (d_2 and d_2). (The peaks of Mo and S elements are overlapped in the EDS spectrum, thus, two spectra containing Mo and S elements were saved for each sample in the measuring process, respectively.)

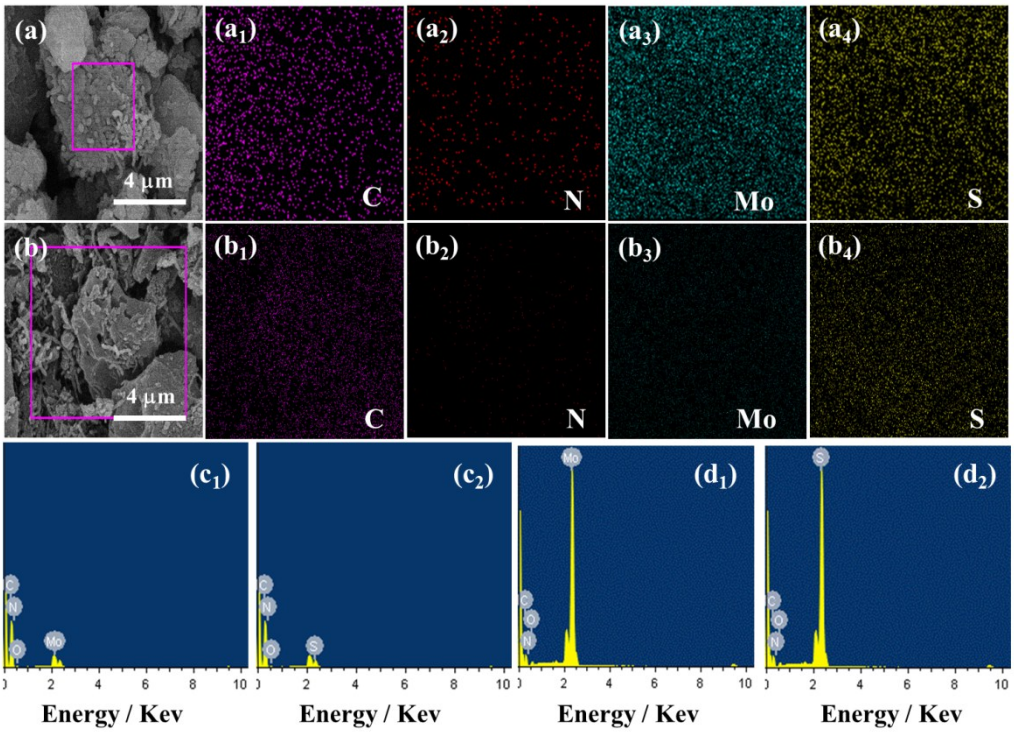

Fig. S2. FESEM image of FSC/MoS_2/CNTs (a) and the corresponding elemental mappings of C, N, Mo and S (a_1-a_4); FESEM image of FSC/MoS_2/CNTs@S (b) and the corresponding elemental mappings of C, N, Mo and S (b_1-b_4); EDS spectra of FSC/MoS_2/CNTs ($c_1$and c_2) and FSC/MoS_2/CNTs@S (d_2 and d_2). (The peaks of Mo and S elements are overlapped in the EDS spectrum, thus, two spectra containing Mo and S elements were saved for each sample in the measuring process, respectively.)

Table S1. The content and peak position of C, N and O of FSC in XPS spectrum.

Element	C	N	O
Content (at %)	94.70	2.31	2.99
Content (wt %)	93.41	2.66	3.93
Peak position (eV)	285.08	396.08	532.08

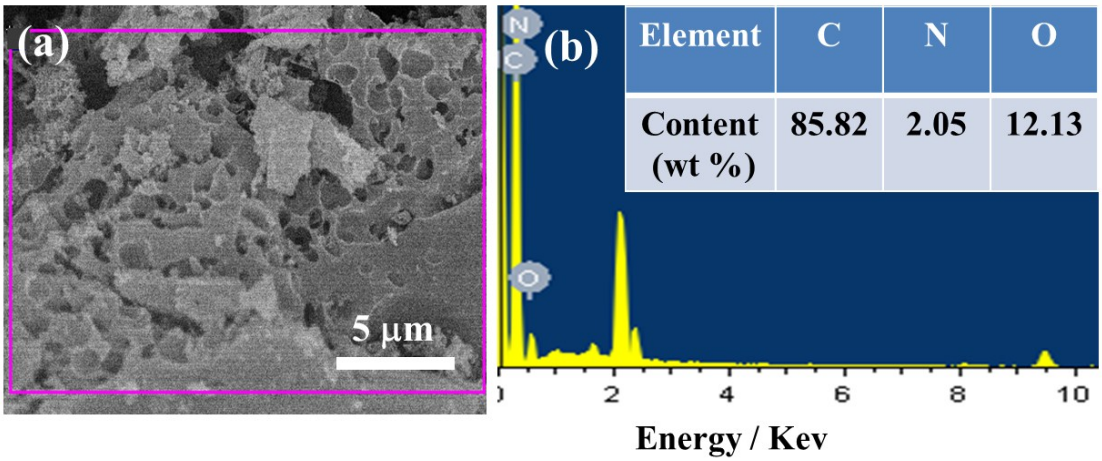

Fig. S3. FESEM image (a) and the corresponding EDS spectrum (b) of FSC.

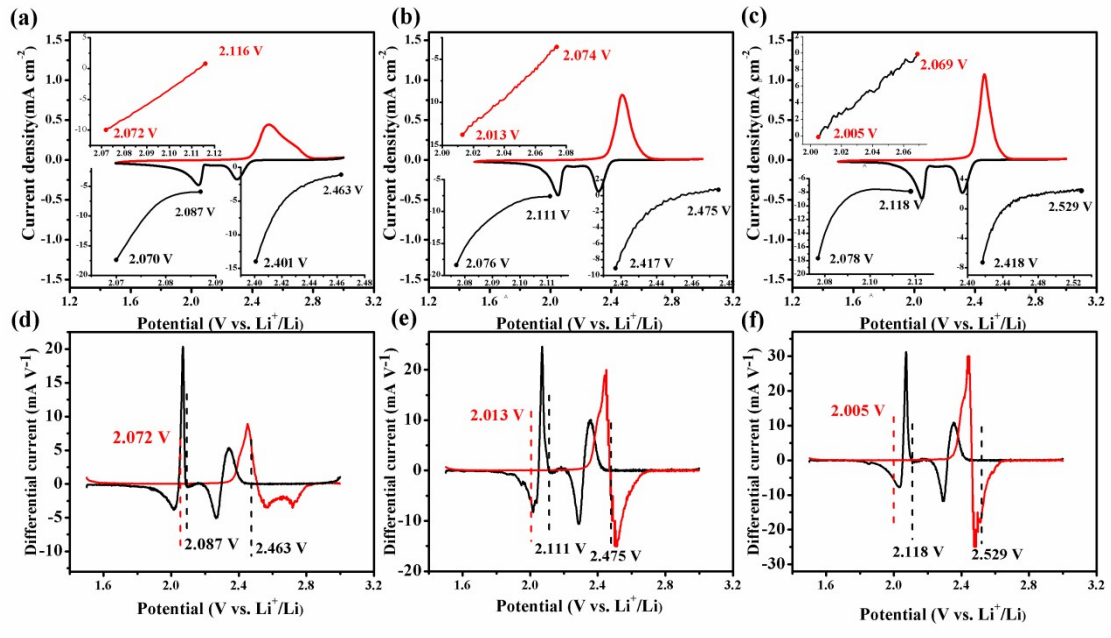

Fig. S4. CV curves and corresponding onset potentials of redox peaks of (a) FCS@S, (b) FCS/MoS_2@S and (c) FCS/MoS_2/CNTs@S cathodes. Differential CV curves of (e) FCS@S, (f) FCS/MoS_2@S and (g) FCS/MoS_2/CNTs@S cathodes. The baseline potential and baseline current density are defined as the value before the redox peak, where the variation on current density is the smallest, namely $dI / dV = 0$.

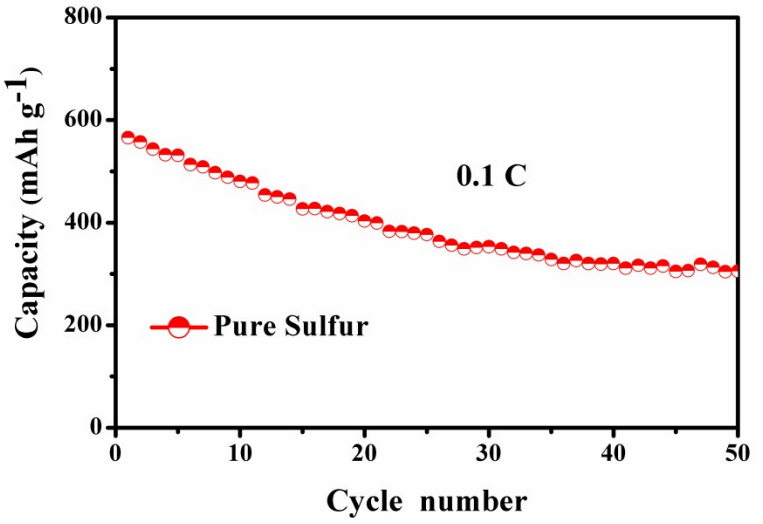

Fig. S5. Cycling performance of pure sulfur electrode at 0.1 C for 50 cycles.

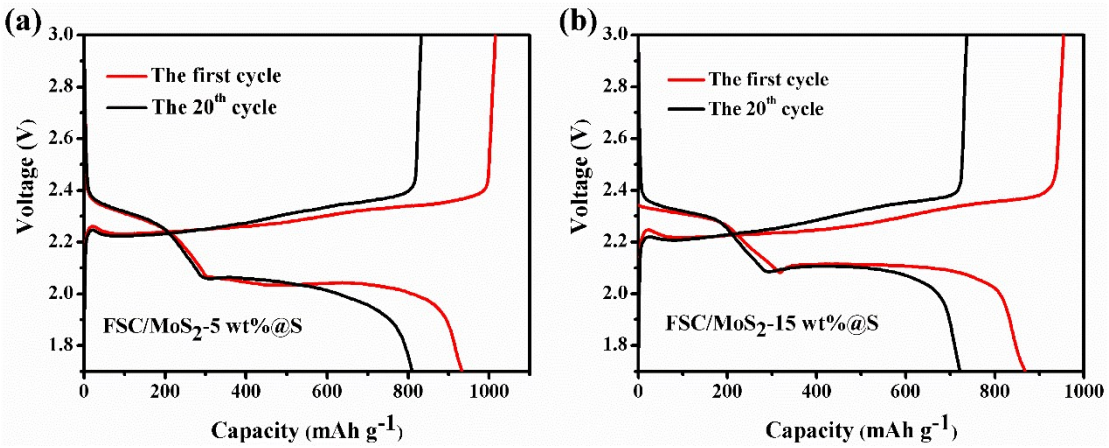

Fig. S6. The first and 20th charge/discharge profiles of (a) FSC/MoS_2-5 wt%@S and (b) FSC/MoS_2-15 wt%@S cathodes at 0.1 C.

For the FSC/MoS_2 sample, the mass ratio of MoS_2 to FSC is calculated to be about 10 wt%. To explore the appropriate content of MoS_2 as inorganic polar additive, the samples with low (~ 5 wt%) and high (~ 15 wt%) mass ratio of MoS_2 to FSC have been also designed by adjusting the weight of $Na_2MoO_4{\cdot}2H_2O$ and CH_4N_2S in proportion. The FSC/MoS_2-5 wt% and FSC/MoS_2-15 wt% samples were obtained based on the same synthetic method as FSC/MoS_2, respectively. The first discharge specific capacities of the FSC/MoS_2-5 wt%@S and FSC/MoS_2-15 wt%@S electrodes are 932.6 and 868.2 mAh g^{-1} at 0.1 C. After 20 cycles, the two electrodes deliver the capacities of 832.1 and 721.8 mAh g^{-1}, respectively. It can be clearly found that the discharge specific capacities of FSC/MoS_2-5 wt%@S and FSC/MoS_2-15 wt%@S electrodes are lower than the FSC/MoS_2 electrode. The possible reason is that too little content of MoS_2 may not play an effective role for improving the performance, while excess MoS_2 may lower the conductivity of the electrode and thus lead to the poor the performance.